Accepted Version

Loss of host type-I IFN signaling accelera es metastasis and impairs NK cell anti-tumor function in multiple models of breast cancer

Jai Rautela[1-3#], Nikola Baschuk[1#], Clare Y. Slaney[1-3], Krishnath M. Jayatilleke[1], Kun Xiao[1], Bradley N. Bidwell[2], Erin C. Lucas[2], Edwin D. Hawkins[2], Peter Lock[1], Christina S. Wong[7], Weisan Chen[1], Robin L. Anderson[2,3,5], Paul J. Hertzog[6], Daniel M. Andrews[2,4], Andreas Möller[7] and Belinda S. Parker[1].

[1]Department of Biochemistry and Genetics, La Trobe Institute for Molecular Science, La Trobe University, Melbourne, Victoria, Australia

[2]Peter MacCallum Cancer Centre, Melbourne, Victoria, Australia

[3]Sir Peter MacCallum Department of Oncology, University of Melbourne, Parkville, Victoria, Australia.

[4]Cancer Immunology Program, Peter MacCallum Cancer Centre, Melbourne, Victoria, Australia

[5]Department of Pathology, University of Melbourne, Parkville, Victoria, Australia

[6]Centre for Innate Immunity and Infectious Diseases, Monash Institute of Medical Research, Monash University, Clayton, Victoria, Australia

[7]QIMR Berghofer Medical Research Institute, Herston, Queensland, Australia

[#]Authors contributed equally to this manuscript

Key words (5): type-I IFN, breast cancer, bone metastasis, immune regulation, NK cells

Financial support: This work was supported by grant funding from the Cancer Council Victoria (BSP and PJH), the National Health and Medical Research Council (NHMRC) (BSP and PJH), fellowship support from NHMRC and ARC (BSP, PJH), the National Breast Cancer Foundation (NBCF) (fellowships to CYS (co-funded by Cure Cancer Australia), RLA and AM).

Corresponding author:
Dr. Belinda S Parker
La Trobe Institute for Molecular Science
La Trobe University, Melbourne, 3086, Australia
Belinda.Parker@latrobe.edu.au

Word count: (4835 including abstract)

Metastatic progression is the major cause of breast cancer related mortality. By examining multiple syngeneic preclinical breast cancer models in mice lacking a functional type-I interferon receptor (Ifnar1$^{-/-}$ mice), we show that host-derived type-I interferon (IFN) signaling is a critical determinant of metastatic spread that is independent of primary tumor growth. In particular, we show that bone metastasis can be accelerated in Balb/c Ifnar1$^{-/-}$ mice bearing either 4T1 or 66cl4 orthotopic tumors and, for the first time, present data showing the development of bone metastasis in the C57Bl/6 spontaneous MMTV-PyMT-driven model of tumorigenesis. Further exploration of these results revealed that endogenous type-I IFN signaling to the host haematopoietic system is a key determinant of metastasis-free survival and critical to the responsiveness of the circulating NK cell population. We find that *in vivo* stimulated NK cells derived from WT, but not Ifnar1$^{-/-}$ mice can eliminate the 4T1 and 66cl4 breast tumor lines with varying kinetics *in vitro*. Together, this study indicates that the dysregulated immunity resulting from a loss of host type-I IFN signaling is sufficient to drive metastasis, and provides a rationale for targeting the endogenous type-I IFN pathway as an anti-metastatic strategy.

Introduction

Metastasis is the deadliest result of malignant disease. Standard clinical practice to avoid this outcome focuses on primary tumor treatment using chemotherapy, radiotherapy and/or surgical resection. However, despite the obvious benefits of these interventions, it has been reported that tumor cell dissemination can occur prior to primary tumor diagnosis (1). It is therefore important to understand the processes that dictate the survival and outgrowth of these disseminated cells to guide the development of novel anti-metastatic therapies. Work on the later stages of the metastatic cascade has uncovered numerous mechanisms of disseminated tumor cell survival and outgrowth, such as resisting apoptosis following detachment from the extra-cellular matrix (2), de-novo angiogenesis (3) and growth factor signaling pathways that promote the proliferation of disseminated cells (4). Many of these mechanisms appear unique to a specific metastatic site, supporting the well-established idea that the organotropism of certain cancers relies upon a favorable interaction between the tumor cell and target microenvironment (5).

Recently, the anti-tumor immune response has emerged as a key factor in determining metastatic spread. Tumor cells can employ multiple immune-evasive tactics to survive at various metastatic sites (6), including our recent findings that show a requirement for breast tumor cells to suppress their innate type-I interferon (IFN) pathway to colonize the bone (7). The type-I IFN family was originally characterized as a group of soluble factors produced by almost all cells in the body that were able to confer an anti-viral state (8, 9). Our knowledge of these cytokines has since broadened to include their ability to directly inhibit the proliferation of various malignant cells and also to induce anti-tumor immune responses (10, 11). Although IFN therapies have had mixed success in the clinic as direct tumoricidal agents, their involvement in tumor immune surveillance is currently the focus of much research. Of particular note, experiments with mice lacking a functional type-I IFN receptor (Ifnar1$^{-/-}$ mice) have demonstrated that endogeneous IFN signaling to the host hematopoietic system is critical for mounting an immunological response against chemically induced sarcomas (12). However, less is known about the role that type-I IFNs play during the anti-metastatic immune response, especially in immune-competent models of breast cancer.

In line with our previous work (7), we hypothesized that if type-I IFN signaling was a critical regulator of breast cancer progression, then blocking such signaling should be sufficient to drive metastasis irrespective of an impact on primary tumor growth. To address this, we studied the full course of disease in a model of spontaneous breast tumorigenesis (MMTV-PyMT) as well as in two orthotopic models (4T1 & 66cl4) of breast cancer metastasis in wild type (WT) and Ifnar1$^{-/-}$ mice. We show model-specific differences in primary tumor growth and lung metastasis, and uncover a common theme of accelerated bone metastasis in Ifnar1$^{-/-}$ mice—a critical site of tumor cell dormancy and relapse in breast cancer patients (13). In addition, we demonstrate that these differences in metastatic spread may be partly attributable to the functionality of the natural-killer (NK) cell component of the host's innate lymphoid population (14). Finally, this work shows a critical role for type-I IFN signaling in

promoting the anti-metastatic response, and highlights the importance of examining the full course of disease when investigating tumor immunity.

Materials and Methods

Mouse models and cell lines

All animal procedures were conducted in accordance with the Australian National Health and Medical Research regulations on the use and care of experimental animals, and approved by the La Trobe Animal Experimentation Ethics Committee. C57Bl/6 MMTV-PyMT mice (15) and C57Bl/6 Ifnar1$^{-/-}$ mice (16, 17) were used to generate C57Bl/6 PyMT-Ifnar1$^{-/-}$ and PyMT-Ifnar1 wild type (WT) mice. BALB/c Ifnar1$^{-/-}$ mice have been described before (17).

The 4T1 and 66cl4 tumor cell lines were sourced directly from Fred Miller who derived the cell lines from a spontaneous mammary tumor that arose in a Balb/c mouse (18). The highly bone-metastatic 4T1.2 sub-clone of the 4T1 line was derived in, and sourced from, Prof. Anderson's laboratory (19). All cells were engineered to express the mCherry and/or Luciferase (Luc2) reporter genes through retroviral transduction (MSCV). The use of the Yac-1 murine leukemia cell line as a robust NK-cell target has been well established (20). All cell lines were cultured in α-MEM (5% FBS) except for the Yac-1 line that was grown in DMEM (10% FBS, non-essential amino acids, sodium pyruvate and L-glutamine) (all Gibco reagents). All adherent cells were passaged using EDTA (0.01% w/v in PBS) and were cultured for no longer than 4 weeks.

Orthotopic tumor cell inoculation, tumor measurement and *ex-vivo* imaging

Single-cell suspensions of 1×10^5 4T1, 4T1.2 or 66cl4 tumor cells in PBS were injected into the 4th mammary gland of 8-12 week old female BALB/c mice. Primary tumor size was measured three times per week using electronic calipers and tumor volume (mm^3) was calculated as L (mm) x W (mm)^2 /2. If indicated, primary tumors were resected when the tumor volume reached 500 mm^3 or in the case of some 66cl4 experiments, at 21 days post tumour cell inoculation. Mice were sacrificed upon signs of metastatic distress or when the cumulative primary tumor volume reached 1500 mm^3. The extent of metastasis in particular organs was assessed using quantitative real-time PCR (qPCR) or visualized by histology as described below. In addition, some organs were rapidly excised from euthanized animals and subjected to *ex vivo* imaging using an IVIS Lumina XR-III (Caliper Life Sciences, Australia). Spectrally un-mixed mCherry fluorescence or bioluminescent intensity 10 minutes after I.P. injection of 1.5 mg D-Luciferin (Gold Biotechnology, USA) were normalized between all images in a group using Living Image 4.4 software (Caliper Life Sciences).

NK cell transfer & metastasis assay

Ifnar1$^{-/-}$ hosts (5 – 6 per group) bearing orthotopic 4T1 tumors were I.V. infused with 300,000 (in 200μL PBS-/-) immunomagnetically purified NK cells (as described in NK isolation methods below) from pooled splenocytes from three poly(I:C)-activated (250ug I.P., 48 hours

prior to isolation) WT or Ifnar1$^{-/-}$ donors on days 2, 7, 17 and 25 post tumor cell inoculation. Primary tumors were resected on day 15 and mice were harvested 31 days post tumour cell inoculation with organs collected for metastatic burden analysis via qPCR as described below.

Quantification of metastatic burden

Duplex qPCR was used to quantify metastatic burden (as previously described by Eckhardt *et. al.* (21)) by comparing the ratio of mCherry (present in tumor cells) and vimentin (NC_000068, present in all cells) sequences in genomic DNA preparations from homogenized and proteinase-K (100 µg/mL, 70663, Merck) digested lungs, spines and femurs. Taqman reagents and StepOne plus instrument were from Applied Biosystems (Life Technologies, Australia) and primers were as follows: mCherry fwd: 5′-GACCACCTACAAGGCCAAGAAG-3′, rev: 5′-AGGTGATGTCCAACTTGATGTTGA-3′, hydrolysis probe: 5′FAM-CAGCTGCCCGGCGCCTACA-3′TAMRA and vimentin fwd: 5′-AGCTGCTAACTACCAGGACACTATTG-3′, rev: 5′-CGAAGGTGACGAGCCATCTC-3′, hydrolysis probe: 5′VIC-CCTTCATGTTTTGGATCTCATCCTGCAGG-3′TAMRA. Assessment of metastatic burden in the spontaneous MMTV-PyMT model required the analysis of PyMT mRNA expression levels in frozen, crushed tissues. RNA was isolated from tissues using Qiagen RNeasy kits (Qiagen, Australia) and 1 µg of RNA was reverse transcribed using the Moloney murine leukaemia virus reverse-transcriptase enzyme (MoMuLV-RT, Promega) and anchored oligo-(dT) primers. PyMT cDNA abundance was quantified relative to the Rps27a housekeeping gene using the previously mentioned Taqman reagents and instrument with the following primers: PyMT fwd: 5′-CCAACAGATACACCCGCACAT-3′, rev: 5′-GGTCTTGGTCGCTTTCTGGATA-3′, hydrolysis probe: 5′FAM-CCCGATGACAGCATAT-3′MGB. Rps27a was measured using a commercial gene expression assay (Life Technologies, cat.# Mm01180369_g1). Gene expression / metastatic burden (arbitrary units) was based on the quantification cycle (C_q) for PyMT relative to Rps27a or mCherry relative to vimentin and displayed as relative tumor burden (RTB) using the following equation:

RTB = 10,000/($2^{\Delta C_q}$), where $\Delta C_q = C_q$(target gene) – C_q(control).

Histology and immunohistochemistry (IHC)

Prior to paraffin embedding and sectioning, all tissues were fixed in 10% neutral buffered formalin for 24 hours. Bone was decalcified in 20% EDTA (pH 8) for two weeks at room temperature after fixation. Cellular morphology was visualized by haemotoxylin and eosin staining (H&E). IHC detection of epithelial cells was used to confirm the presence of bone metastases with a previously described protocol (7). Briefly, tissues were subjected to heat-induced epitope retrieval (125°C for 3 min under pressure) in citrate buffer (10 mM sodium citrate, pH 6) before incubating with a pan anti-cytokeratin antibody (5 µg/mL, 4°C overnight) that recognizes cytokeratins 5, 6 and 8 (clone PCK-26, Abcam, USA).

Immuno blot and ELISA techniques

Standard western blotting and SDS-PAGE protocols were used to prepare and separate samples on 4-20% acrylamide gels. Membranes were gently agitated at 4°C overnight in a 5% skim-milk solution containing antibodies against murine Irf7 (AbD Serotec, AHP1180, 1 µg / mL) or GAPDH (cell signaling, #8884, 1:5,000 dilution). Primary antibody binding was detected using an anti-rabbit HRP-conjugated secondary antibody (raised in donkey) and visualized using ECL substrate (Amersham ECL Prime, GE healthcare) and a digital image capture system (Syngene, In Vitro Technologies, Australia). Measurement of IFNα secretion was performed by plating 25,000 cells of interest in triplicate wells of a 96-well-plate which were allowed to adhere overnight before transfecting (Lipofectamine 2000, Invitrogen) with 10 µg / mL poly(I:C) for 6 hours. Transfection media was then carefully aspirated and replaced with 50 µL of complete growth media and allowed to incubate for 16 – 18 hours 37°C / 5% CO_2. Standard ELISA protocols were then used to detect IFNα secretion, briefly, 35 µL of cell-free supernatant was then transferred to immunoassay plates coated with mIFNa capture antibody (1:500, 22100-1 / RMMA-1, PBL assay sciences), incubated for 2 hours at RT before sequential incubations with mIFNa anti-serum (1:500, 32100-1, PBL biosciences), anti-rabbit-HRP tertiary antibody (1:500), TMB substrate (Sigma-Aldrich) for 30 min at RT before quenching the reaction and measuring the OD at 450nm with λ correction at 570nm.

Flow cytometric analysis

Analysis of blood immune cell populations was completed by flow cytometry using an LSR-II and FACSCanto II (BD Biosciences, USA) and data were analyzed using Flowjo software (Tree Star, USA). Blood from the lateral tail-vein was used to profile the circulating immune populations after red blood cell lysis (155mM NH_4Cl, 10mM $KHCO_3$, 0.1mM EDTA, pH 7.3) and staining with the following antibodies: CD11b-FITC (M1/70), CD8a-PerCP (53-6.7), CD4-APC (RM4-5), TCRβ-FITC (H57-597), NKp46-BV421 (29A1.4), Ly6G-BV421 (1A8), Ly6C-APC (HK1.4), CD69-PE (H1.2F3) (all from BD Biosciences, San Diego, CA, USA). Intracellular IFN-γ accumulation was analyzed using a specially designed kit (554715, BD Biosciences) according to the manufacturer's instructions after cells were stimulated with 20 ng/ml PMA and 1 µg/ml Ionomycin for 4 hr in the presence of Golgi stop. For the analysis of NK cell ligands and the Ifnar1 receptor present on the tumor cell surface, the following antibodies were used: H2D(d)-PE (34-5-8S), H2K(d)-FITC (SF1-1.1) (BD Biosciences), CD155-PE (TX56), Ifnar1-PE (MAR1-5A3) (Biolegend, San Diego, CA, USA) and MULT1-PE (237104), pan-Rae-1-PE (186107) and H60-APC (205326) (R&D Systems, Minneapolis, MN, USA).

NK cell isolation & Cytotoxicity assays

Standard 4 hr cytotoxicity assays were completed as described elsewhere (22). Briefly, splenic NK cells from naïve or poly(I:C) activated (250 µg I.P. 48 hr prior to isolation) WT, $Ifnar1^{-/-}$ or animals injected with an Ifnar1 blocking antibody (MAR1-5A3, 200 µg I.P., 72, 48 and 24 hours prior to harvest) were immunomagnetically enriched (NK cell enrichment kit,

#19755, Stem Cell Technologies, Australia) according to manufacturer's specifications and suspended in complete NK cell medium (phenol-red free RPMI 1640 containing: 10% FBS, β-Me, non-essential amino acids, L-glutamine, sodium pyruvate, all from Gibco). The indicated target cells were labelled with 15 μM calcein-AM (C3099, Life Technologies) for 30 min at 37°C, washed thrice and also suspended in NK cell medium. Effector and target cells were combined at the indicated ratios in triplicate wells of a round-bottom 96 well plate and incubated at 37°C / 5% CO_2 for 4 or 18 hours. Calcein release was quantified by transferring 100 μL of cell-free supernatant to opaque 96 well plates and measuring fluorescent emission at the appropriate wavelength (excitation filter: 485±9 nm; cutoff: 515 nm; emission: 525±15 nm) using a Spectramax M5e microplate reader (Molecular Devices, Sunnyvale, Calif.). Plates were then stored at -20°C for subsequent CBA cytokine analysis as described below. Cytotoxicity data were expressed as percent lysis relative to the spontaneous (target cells alone) and maximum release (1% triton X-100 treated cells) for a particular target with the equation: % lysis = ((sample – spontaneous) / (maximum – spontaneous)) * 100

Apoptosis and proliferation assays

66cl4 and NK cell co-cultures were set up as described above, incubated for 18 hours and stained in Annexin-V binding buffer (556454, BD Biosciences) containing TO-PRO-3 (500 nM, T3605, Life Technologies) and Annexin-V-FITC (556419, BD Biosciences) according to manufacture's specifications. Samples were analyzed using a FACS ARIA III cell sorter (BD Biosciences) equipped with a 561 nm laser to optimally resolve the mCherry positive tumor cells and ensure that the resulting profiles did not represent apoptotic leukocytes. Proliferation assays were performed in the presence of 1000 I.U. / mL mIFNα or β (produced in-house) as previously described(21) using sulforhodamine-B binding assays.

Bone marrow reconstitution

Female BALB/c mice (6-8 weeks old) received two doses of 5.5 Gy irradiation 3.5 hours apart before an intravenous injection of 2×10^6 bone marrow cells isolated from 6-8 week old BALB/c WT or Ifnar1$^{-/-}$ mice. Six weeks later, reconstitution was confirmed by flow cytometric analysis (FACS) of Ifnar1 expression on blood cells (Ifnar1 antibody clone: MAR1-5A3). Ten weeks after reconstitution, recipients were inoculated with 4T1.2 tumor cells as described above. Subsequent to tumor resection, mice were monitored daily until each individual mouse showed signs of distress due to metastatic burden.

Statistical analysis

Differences in primary tumor size and immune populations were assessed with Student's *t*-tests and metastasis assays (non-normally distributed data) were analyzed with Mann-Whitney U-tests. Mantel-Cox log-rank tests were used to evaluate differences in metastasis-free survival. ELISA data were interpolated from a 4-paramater logistic regression of a standard curve using a free online program available at: ElisaAnalysis.com (Leading

Technology Group, Australia). GraphPad Prism software (GraphPad, USA) was used for all analyses. *P*-values: **P*≤0.05, ***P*<0.005, ****P*<0.0005.

Results & Discussion

Loss of type-I IFN signaling accelerates bone metastasis independent of primary tumor growth.

We initially set out to determine if type-I IFN signaling could impact upon tumor development and metastasis in a model of breast cancer with spontaneous tumor initiation. The tumors that develop in the viral oncogene driven MMTV-PyMT model are thought to faithfully recapitulate the human disease through the stages of early hyperplasia, carcinoma *in situ*, invasive cancer and sporadic pulmonary metastasis (23, 24). Importantly, this model allows the assessment of other factors on tumor initiation, unlike our previous analysis using aggressive transplantable models where type-I IFN signaling did not impact on tumor growth, contrary to other studies with sarcoma models (12). Nevertheless, in line with our previous study (7), crossing these mice to hosts lacking a competent type-I IFN receptor (PyMT-Ifnar1$^{-/-}$ mice) revealed similar tumor growth kinetics for both genotypes (Fig. 1A, B), leading us to conclude that endogenous IFN signaling was not a key regulator of primary tumor initiation or growth of PyMT-driven tumors. Other groups focusing on tumor immunity have also observed a lack of PyMT primary tumor responsiveness to immunological challenge. One such report has shown that although PyMT lung metastasis can be contained by an effective CD8^{+} T cell response, T cell immunity at the primary site was likely dysfunctional due to intense immune suppression (25). These data illustrate an obvious challenge in promoting primary tumor immunity, however, the question of whether a total lack of IFN signaling could sufficiently derail the peripheral anti-tumor immune response to promote metastasis still remains.

The similarities in primary tumor growth regardless of the functional status of the type-I IFN pathway gave us the opportunity to measure the metastasis-specific roles of type-I IFN signaling in MMTV-PyMT mice. Importantly, we observed an increase in bone metastasis as revealed by a significant increase in PyMT tumor burden in the spine (Fig. 1C) (mean RTB for WT cohort = 23.5 and Ifnar1$^{-/-}$ cohort = 155.7), and the rare but histologically detectable development of femur metastasis in PyMT-Ifnar1$^{-/-}$ mice (Fig. 1D, F). This was a bone specific effect, with no change in lung metastasis observed (Fig. 1E). To the best of our knowledge, this report is one of the first studies to show extensive spontaneous bone metastasis using the PyMT model on the C57Bl/6 background. The significance of this finding is further underscored by the fact that these experiments were terminated due to the size of multiple primary tumors, rather than signs of metastatic distress. This reduced the time allowed for metastatic progression and no doubt reduced the frequency of bone metastasis. For this reason, we decided to move to transplantable tumor models to further study the impact of a lack of host type-I IFN signaling on metastasis and breast tumor immunity.

Orthotopic mouse mammary tumor models show distinct patterns of progression in hosts lacking a functional type-I IFN system

To assess the impact of a defective type-I IFN host response on transplantable orthotopic tumors in immunocompetent mice, we chose to use the highly lung metastatic 4T1 and weakly metastatic 66cl4 isogenic cell lines from the Miller series (18). These cell lines form primary tumors and metastasize reliably and predictably in Balb/c mice, allowing for appropriate design of experiments that can dissect the role of type I IFN signaling on tumor growth, metastasis and immune activation.

Our experiments revealed that both models had vastly different patterns of progression depending on the type-I IFN signaling status of the host, and was independent of Ifnar1 expression (Fig. 6A) or intrinsic IFN sensitivity of either cell line (Supp. Fig 4A, B). Indeed both cell lines were able to secrete substantial levels of IFNα upon stimulation (Supp. Fig. 4C) and had similar basal levels of the key interferon-driven transcription factor, Irf7 (Supp. Fig 4D), suggesting that differences in IFN sensitivity or secretion could not account for the differential behavior of these cell lines *in vivo.* The 4T1 model followed a similar mode of progression to PyMT-driven tumors, with primary tumor growth (Fig. 2A) and lung metastasis (Fig. 2B, C) not affected by the IFN signaling status of the host. In contrast, 66cl4 tumors appeared to be highly sensitive to endogenous type-I IFN signaling, such that primary tumor growth and lung metastasis were significantly increased in Ifnar1$^{-/-}$ mice (Fig 2A, B). As this acceleration of lung metastasis was also observable when experiments were controlled for primary tumor size (Fig. 2C), it appeared that Ifnar1$^{-/-}$ mice had a true defect in the anti-metastatic response. Importantly, we found that both the 4T1 and 66cl4 cells more readily metastasized to the spine and femurs in Ifnar1$^{-/-}$ mice (Fig. 3A-C), further strengthening our finding of the critical nature of type-I signaling in regulating bone metastasis.

In light of multiple reports showing tumor immunity in these models (25, 26), and the fact that tonic IFN signaling is required to maintain normal hematopoiesis (27), our data indicate a role for the immune system in regulating metastatic spread. In support of this, the loss of hematopoietic Ifnar1 (by using chimeras made from WT recipients and normal (WT) or IFN-insensitive (Ifnar1$^{-/-}$) bone marrow) reduced metastasis free survival in the 4T1.2 model—an aggressive variant of the 4T1 line—in the absence of an impact on orthotopic tumor growth (Sup. Fig. 1A, B). However, the specific immunological mechanisms responsible for this survival advantage remain unclear.

Type-I IFNs promote NK cell-mediated elimination of breast tumor cells

Homeostasis of the NK cell compartment appears to be particularly dependent upon endogenous type-I IFN signaling, as reports have shown that Ifnar1$^{-/-}$ mice possess a relatively immature pool of these cells (28). Similarly, the dysfunction of the NK cell compartment in Ifnar1$^{-/-}$ null mice has been implicated in the establishment of some tumors (16), and more recent data have proven the importance of these cells in preventing the outgrowth of experimental melanoma metastases (29). We therefore hypothesized that the differences in metastasis between WT and Ifnar1$^{-/-}$ hosts could be due in part to the ability of NK cells to recognize and eliminate the 4T1 and 66cl4 breast tumors.

We therefore measured NK cell number and activation during progression of the transplantable tumors and found an indication that NK cells were responding to the developing tumor. Analysis of circulating NKp46^{+} NK cell proportions in 4T1 and 66cl4 tumor bearing mice indicated an early expansion of this population (Fig. 4A, D), with an increase from 4% to 6% five to seven days post tumor cell inoculation. In support of this NK cell response, we also observed differences in NK cell CD69 expression (an early activation marker) and interferon-gamma (IFNγ) re-stimulation potential in tumor bearing hosts. Importantly, we found that Ifnar1$^{-/-}$ hosts had significantly diminished levels of both of these markers in comparison to WT 4T1-bearing counterparts (Fig. 4B, 4C). A similar (although not significant) trend was also observed in the 66cl4 model (Fig. 4E), though NK cells from WT tumor bearing mice were still able to produce more IFNγ than their naïve counterparts. Together, these data indicate that WT NK cells were responding to the developing cancer but that this response was impaired in Ifnar1$^{-/-}$ hosts.

In addition to this apparent heightened NK cell activity in WT tumor bearing mice, we found that they were also capable of killing mammary tumor lines *in vitro*. Cytotoxicity experiments revealed that *in vivo* activated NK cells purified from WT but not Ifnar1$^{-/-}$ mice (Fig. 5A) or mice administered an Ifnar1 blocking antibody (Fig. 5C) could effectively eliminate 4T1 tumor cells, showing a clear dependency on type-I IFN signaling in arming the cytotoxic response against this line. In contrast, similar experiments with the 66cl4 line showed an apparent resistance to cytotoxicity, irrespective of whether the NK cells were derived from WT or Ifnar1$^{-/-}$ hosts (Fig. 5B). Although these data were somewhat at odds with the relative metastatic ability of each tumor model, these findings highlight the critical importance of using the cell type under investigation as the target in such cytotoxicity assays. Many other studies likely miss these nuances by correlating NK cell cytotoxicity with highly susceptible target cells (such as the Yac-1 line we used as experimental controls in Fig. 5B). In addition, cytotoxicity assays reported in the literature commonly use high concentrations of cytokines, such as IL-2, to expand and activate the population beyond what would be physiologically reasonable, masking the impact of IFN signaling and target-specific sensitivities to NK cell attack. Indeed, under these hyper-activating conditions, we have previously observed no difference in cytotoxic ability between NK cells derived from WT and Ifnar1$^{-/-}$ mice, and even lysis of the apparently resistant 66cl4 line (Sup. Fig 2). Therefore, our approach of dosing mice with poly(I:C) (a well-characterized IFN-agonist (30)), allowing *in vivo* activation and using NK cells immediately after isolation were ideal experimental conditions to examine type-I IFN-mediated cytotoxicity against our tumor lines.

Given the apparent susceptibility of the 4T1 cell line to NK-mediated cytotoxicity *in vitro,* we conducted NK cell therapy experiments to understand whether adoptive transfer of this immune cell type alone could restrain metastatic spread. Ifnar1$^{-/-}$ hosts were chosen due to the enhanced rate of bone metastasis seen in these mice and to negate the contribution of endogenous IFN signaling to the immune system. 4T1 tumor bearing hosts were then intravenously infused with NK cells purified from poly(I:C) stimulated WT or Ifnar1$^{-/-}$ donors at

two time points prior to tumour resection and twice post surgery. In accordance with our other 4T1 tumour growth data (Fig. 2A), the infusion of NK cells from either donor genotype did not impact primary tumour growth (Fig. 5D). In order to provide a reference for data distribution, we overlaid metastasis data gathered from these NK cell transfer experiments (Fig. 5E, F, black points) on our previous 4T1 metastasis data (from Fig. 2B, 3A, grey points). These comparisons clearly show that the transfer of WT or Ifnar1$^{-/-}$ donors did not impact metastatic burden in the lung (Fig. 5E), however, there was a clear reduction in spine metastasis observed in Ifnar1$^{-/-}$ mice infused with activated WT NK cells (Fig. 5F) that correlated with reduced spine metastasis in WT animals (Fig. 3A or Fig. 5F grey points). Although this impact on spine metastasis did not reach the traditional cutoffs of significance using standard statistical tests (perhaps due to the small experimental cohort), it does suggest a role for NK cells in conferring anti-metastatic protection in the bone.

We next investigated the apparent paradox between NK susceptibility and metastatic potential. As NK cell recognition is known to depend on the net signaling outcome from both activating and inhibitory receptors (31), we wondered whether the expression of their cognate ligands on the tumor cell surface would correlate with our cytotoxicity assays. We found that levels of MHC class-I molecules recognized by Ly49 family of inhibitory NK cell receptors were expressed at higher levels on 66cl4 cells relative to 4T1 cells (Fig. 6A). Although the activation and release of cytotoxic granules from NK cells is known to be dependent upon multiple signaling inputs (32), it is plausible that this difference in MHC class-I contributed to the susceptibility of 4T1 but not 66cl4 cells to rapid cytotoxic attack. However, we wondered whether 66cl4 cells could eventually succumb to NK cell mediated death if the period of co-culture was increased. We therefore performed overnight cytotoxicity experiments and found that 66cl4 cells could indeed be killed by WT but not Ifnar1$^{-/-}$ NK cells (Fig. 6B), and that the proportion of apoptotic 66cl4 cells was greater when co-cultured with WT NK cells (Fig. 6C). Although further elucidation of this mechanism was beyond the scope of this study, it is well known that NK cells can engage distinct modes of cytotoxicity that have variable kinetics of inducing target cell death (33). Together, the data presented indicate that type-I IFN signaling can have a broad impact on NK-mediated immune surveillance mechanisms.

Finally, we cannot rule out a contribution of the adaptive immune system to this IFN-linked anti-metastatic response. Type-I IFNs are well known to support the expansion (34) and maintenance of activated CD8^{+} T cells (35). This, along with our observation of elevated T cell number in WT hosts bearing 66cl4 tumors (Sup. Fig. 3), would suggest some involvement of the adaptive immune system. Interestingly, one very recent study has integrated our findings by reporting that NK cells may contribute to tumor immunity by promoting antigen cross-presentation (36). This suggests that some of the roles NK cells play during anti-tumor immunity may be independent of their cytotoxic function. Thus, in addition to closer examination of the adaptive immune response in these models, future studies will need to further investigate the relative contribution of NK cells to the global anti-metastatic

response—perhaps through the use of recently published models of innate immunodeficiency (29).

Concluding remarks

Models of spontaneous breast cancer bone metastasis are rare. In this study we have demonstrated that three non-bone metastatic breast tumor models can successfully colonize the bone in hosts with a defective type-I IFN pathway—underscoring the importance of IFN signaling during the anti-metastatic response. An interesting area to investigate in the future will be how the bone-resident immunity (37) differs in relation to other metastatic sites, and why tumors that induce large numbers of circulating suppressive cells fail to metastasise to this organ without the loss of type-I IFN signaling. Indeed, MDSC accumulation has been implicated with 'pre-metastatic niche' formation in the lung (38), which may explain why lung metastasis was not consistently enhanced by a loss of IFN signaling. Also on the theme of site-specific immunity, it will be important to investigate whether differences in resident immune populations (such as the emerging picture of distinct NK cell populations (39, 40)) are responsible for the discrete patterns of metastasis of some cancers. Finally, our data show a potential role for NK cells to engage in the anti-metastatic immune response, though it is unclear whether this population can gain sufficient stimulation during cancer progression to effectively eliminate disseminated cells. As some studies have reported a general decrease in NK functionality during breast tumor progression (41), IFN-based therapies aimed at re-activating these cells may prove beneficial as novel anti-metastatic therapies.

Bibliography:

1. Klein CA. Parallel progression of primary tumours and metastases. Nat Rev Cancer. 2009;9:302-12.
2. Liotta LA, Kohn E. Anoikis: cancer and the homeless cell. Nature. 2004;430:973-4.
3. Holmgren L, O'Reilly MS, Folkman J. Dormancy of micrometastases: balanced proliferation and apoptosis in the presence of angiogenesis suppression. Nat Med. 1995;1:149-53.
4. Yin JJ, Selander K, Chirgwin JM, Dallas M, Grubbs BG, Wieser R, et al. TGF-beta signaling blockade inhibits PTHrP secretion by breast cancer cells and bone metastases development. J Clin Invest. 1999;103:197-206.
5. Fidler IJ. The pathogenesis of cancer metastasis: the 'seed and soil' hypothesis revisited. Nat Rev Cancer. 2003;3:453-8.
6. Slaney CY, Rautela J, Parker BS. The emerging role of immunosurveillance in dictating metastatic spread in breast cancer. Cancer Res. 2013;73:5852-7.
7. Bidwell BN, Slaney CY, Withana NP, Forster S, Cao Y, Loi S, et al. Silencing of Irf7 pathways in breast cancer cells promotes bone metastasis through immune escape. Nat Med. 2012;18:1224-31.
8. Isaacs A, Lindenmann J. Virus interference. I. The interferon. Proc R Soc Lond B Biol Sci. 1957;147:258-67.
9. Nagano Y, Kojima Y. [Inhibition of vaccinia infection by a liquid factor in tissues infected by homologous virus]. C R Seances Soc Biol Fil. 1958;152:1627-9.
10. Gresser I, Maury C, Brouty-Boye D. Mechanism of the antitumour effect of interferon in mice. Nature. 1972;239:167-8.
11. Balkwill F, Watling D, Taylor-Papadimitriou J. Inhibition by lymphoblastoid interferon of growth of cells derived from the human breast. Int J Cancer. 1978;22:258-65.
12. Dunn GP, Bruce AT, Sheehan KC, Shankaran V, Uppaluri R, Bui JD, et al. A critical function for type I interferons in cancer immunoediting. Nat Immunol. 2005;6:722-9.
13. Braun S, Vogl FD, Naume B, Janni W, Osborne MP, Coombes RC, et al. A pooled analysis of bone marrow micrometastasis in breast cancer. N Engl J Med. 2005;353:793-802.
14. Spits H, Artis D, Colonna M, Diefenbach A, Di Santo JP, Eberl G, et al. Innate lymphoid cells--a proposal for uniform nomenclature. Nat Rev Immunol. 2013;13:145-9.
15. Davie SA, Maglione JE, Manner CK, Young D, Cardiff RD, MacLeod CL, et al. Effects of FVB/NJ and C57Bl/6J strain backgrounds on mammary tumor phenotype in inducible nitric oxide synthase deficient mice. Transgenic Res. 2007;16:193-201.
16. Swann JB, Hayakawa Y, Zerafa N, Sheehan KC, Scott B, Schreiber RD, et al. Type I IFN contributes to NK cell homeostasis, activation, and antitumor function. J Immunol. 2007;178:7540-9.
17. Hwang SY, Hertzog PJ, Holland KA, Sumarsono SH, Tymms MJ, Hamilton JA, et al. A null mutation in the gene encoding a type I interferon receptor component eliminates antiproliferative and antiviral responses to interferons alpha and beta and alters macrophage responses. Proc Natl Acad Sci U S A. 1995;92:11284-8.

18. Aslakson CJ, Miller FR. Selective events in the metastatic process defined by analysis of the sequential dissemination of subpopulations of a mouse mammary tumor. Cancer Res. 1992;52:1399-405.
19. Lelekakis M, Moseley JM, Martin TJ, Hards D, Williams E, Ho P, et al. A novel orthotopic model of breast cancer metastasis to bone. Clin Exp Metastasis. 1999;17:163-70.
20. Quan PC, Ishizaka T, Bloom BR. Studies on the mechanism of NK cell lysis. J Immunol. 1982;128:1786-91.
21. Eckhardt BL, Parker BS, van Laar RK, Restall CM, Natoli AL, Tavaria MD, et al. Genomic analysis of a spontaneous model of breast cancer metastasis to bone reveals a role for the extracellular matrix. Mol Cancer Res. 2005;3:1-13.
22. Neri S, Mariani E, Meneghetti A, Cattini L, Facchini A. Calcein-acetyoxymethyl cytotoxicity assay: standardization of a method allowing additional analyses on recovered effector cells and supernatants. Clin Diagn Lab Immunol. 2001;8:1131-5.
23. Guy CT, Cardiff RD, Muller WJ. Induction of mammary tumors by expression of polyomavirus middle T oncogene: a transgenic mouse model for metastatic disease. Mol Cell Biol. 1992;12:954-61.
24. Lin EY, Jones JG, Li P, Zhu L, Whitney KD, Muller WJ, et al. Progression to malignancy in the polyoma middle T oncoprotein mouse breast cancer model provides a reliable model for human diseases. Am J Pathol. 2003;163:2113-26.
25. Eyob H, Ekiz HA, Derose YS, Waltz SE, Williams MA, Welm AL. Inhibition of ron kinase blocks conversion of micrometastases to overt metastases by boosting antitumor immunity. Cancer Discov. 2013;3:751-60.
26. Olkhanud PB, Baatar D, Bodogai M, Hakim F, Gress R, Anderson RL, et al. Breast cancer lung metastasis requires expression of chemokine receptor CCR4 and regulatory T cells. Cancer Res. 2009;69:5996-6004.
27. Gough DJ, Messina NL, Clarke CJ, Johnstone RW, Levy DE. Constitutive type I interferon modulates homeostatic balance through tonic signaling. Immunity. 2012;36:166-74.
28. Mizutani T, Neugebauer N, Putz EM, Moritz N, Simma O, Zebedin-Brandl E, et al. Conditional IFNAR1 ablation reveals distinct requirements of Type I IFN signaling for NK cell maturation and tumor surveillance. Oncoimmunology. 2012;1:1027-37.
29. Sathe P, Delconte RB, Souza-Fonseca-Guimaraes F, Seillet C, Chopin M, Vandenberg CJ, et al. Innate immunodeficiency following genetic ablation of Mcl1 in natural killer cells. Nature communications. 2014;5:4539.
30. McCartney S, Vermi W, Gilfillan S, Cella M, Murphy TL, Schreiber RD, et al. Distinct and complementary functions of MDA5 and TLR3 in poly(I:C)-mediated activation of mouse NK cells. J Exp Med. 2009;206:2967-76.
31. Lanier LL. NK cell recognition. Annu Rev Immunol. 2005;23:225-74.
32. Long EO, Kim HS, Liu D, Peterson ME, Rajagopalan S. Controlling natural killer cell responses: integration of signals for activation and inhibition. Annu Rev Immunol. 2013;31:227-58.
33. Smyth MJ, Cretney E, Kelly JM, Westwood JA, Street SE, Yagita H, et al. Activation of NK cell cytotoxicity. Mol Immunol. 2005;42:501-10.
34. Curtsinger JM, Valenzuela JO, Agarwal P, Lins D, Mescher MF. Type I IFNs provide a third signal to CD8 T cells to stimulate clonal expansion and differentiation. J Immunol. 2005;174:4465-9.

35. Marrack P, Kappler J, Mitchell T. Type I interferons keep activated T cells alive. J Exp Med. 1999;189:521-30.
36. Deauvieau F, Ollion V, Doffin AC, Achard C, Fonteneau JF, Verronese E, et al. Human natural killer cells promote cross-presentation of tumor cell-derived antigens by dendritic cells. Int J Cancer. 2015;136:1085-94.
37. Baschuk N, Rautela J, Parker BS. Bone specific immunity and its impact on metastasis. BoneKEy. 2015;In press.
38. Sceneay J, Smyth MJ, Moller A. The pre-metastatic niche: finding common ground. Cancer Metastasis Rev. 2013;32:449-64.
39. Andrews DM, Smyth MJ. A potential role for RAG-1 in NK cell development revealed by analysis of NK cells during ontogeny. Immunol Cell Biol. 2010;88:107-16.
40. Karo JM, Schatz DG, Sun JC. The RAG recombinase dictates functional heterogeneity and cellular fitness in natural killer cells. Cell. 2014;159:94-107.
41. Mamessier E, Sylvain A, Thibult ML, Houvenaeghel G, Jacquemier J, Castellano R, et al. Human breast cancer cells enhance self tolerance by promoting evasion from NK cell antitumor immunity. J Clin Invest. 2011;121:3609-22.

Figure legends.

Figure 1.

Ifnar1 deficiency results in accelerated bone metastasis in the spontaneous MMTV-PyMT-driven model of spontaneous tumorigenesis.

(A) Time to palpable tumor development and **(B)** time until maximum ethical tumor volume (1500 mm^3) in MMTV-PyMT WT (n=30) and MMTV-PyMT Ifnar1$^{-/-}$ (n=28) mice was assessed. Subsequent metastatic burden in the **(C)** spine, **(D)** femurs and **(E)** lung of MMTV-PyMT WT (n=22) and MMTV-PyMT Ifnar1$^{-/-}$ (n=20) was quantified using RT-qPCR and expressed as relative tumor burden (RTB). *p < 0.05 using Mann-Whitney U-tests. Error bars represent SEM. **(F)** Representative H&E and pan-cytokeratin (CK) stained femur sections from MMTV-PyMT WT and Ifnar1$^{-/-}$ mice at ethical tumor endpoint. Scale bars represent 50μm.

Figure 2.

4T1 and 66cl4 primary tumor growth and lung metastasis are differentially impacted in hosts with defective type-I IFN signaling.

(A, B) Female age matched WT and Ifnar1$^{-/-}$ mice were injected with 1x10^5 4T1 or 66cl4 tumor cells into the 4th mammary gland and **(A)** primary tumor growth of 4T1-bearing WT (n=7) and Ifnar1$^{-/-}$ (n=10) and 66cl4-bearing WT (n=10) and Ifnar1$^{-/-}$ (n=14) mice was monitored. *p < 0.05 using Student's t-tests. Error bars represent SEM. **(B)** Mice were culled after 32 days (4T1) or 21 days after primary tumor resection (66cl4) to assess metastatic spread. Tumor burden in the lung of 4T1-bearing WT (n=18) or Ifnar1$^{-/-}$ (n=19) mice and 66cl4-bearing WT (n=14) or Ifnar1$^{-/-}$ (n=14) mice were quantified by quantitative real-time PCR and expressed as relative tumor burden (RTB). **p < 0.005 using Mann-Whitney U-tests. Error bars represent SEM. **(C)** Representative ex-vivo bioluminescent (66cl4) and mCherry (4T1) imaging of lungs collected from 4T1-bearing WT and Ifnar1$^{-/-}$ tumor bearing mice 27 days after tumor inoculation. WT (n=4) and Ifnar1$^{-/-}$ (n=4) 66cl4-bearing mice were resected when each individual had an estimated tumor size of 500 mm^3, and culled precisely 36 days post surgery (meaning that WT mice on average had a longer tumor-bearing period).

Figure 3.

Hosts with defective type-I IFN signaling are more susceptible to bone metastasis when bearing orthotopic 4T1 or 66cl4 tumors.

(A-C) Female age matched WT and Ifnar1$^{-/-}$ mice were injected with 1x10^5 4T1 or 66cl4 tumor cells into the 4th mammary gland and mice were culled after 32 days (4T1) or 21 days after primary tumor resection (66cl4) to assess metastatic spread. Metastatic burden in **(A)** spines and **(B)** femurs of 4T1-bearing WT (n=18) or Ifnar1$^{-/-}$ (n=19) mice and 66cl4-bearing WT (n=14) or Ifnar1$^{-/-}$ (n=14) mice were quantified by qPCR and expressed as relative tumor burden (RTB). *p < 0.05, **p < 0.005 using Mann-Whitney U-tests. Error bars represent SEM.

(C) Representative areas of H&E-stained femur sections from WT and Ifnar1$^{-/-}$ mice bearing orthotopic 4T1 and 66cl4 tumors as described above, scale bars represent 50µm**.**

Figure 4.

Impaired functionality of Ifnar1$^{-/-}$ NK cells after orthotopic injection of 4T1 or 66cl4 cells.

(A-C) Female age matched WT (*n*=5) and Ifnar1$^{-/-}$ (*n*=5) mice were injected with 1x10^5 4T1 or **(D, E)** 1x10^5 66cl4 cells into the 4th mammary gland. On indicated days after tumor cell inoculation blood samples were taken and mononuclear cells were immunostained to reveal **(A, D)** the proportion of circulating (NKp46$^+$) NK cells, **(B)** activated (NKp46$^+$/CD69$^+$) NK cells and **(C, E)** NK cell IFNγ production (NKp46$^+$/IFNγ$^+$ cells) by flow cytometery. Naïve NK cell proportions shown in **(A)** are also shared with **(D)**. Data are represented as the proportion of peripheral blood lymphocytes (PBL) and each experiment was repeated twice. **p* < 0.05, ***p* < 0.005, ****p* < 0.0005 using Student's t-tests. Error bars represent SEM.

Figure 5.

The isogenic 4T1 and 66cl4 cell lines are differentially sensitive to NK cell-mediated cytotoxicity.

(A - C) Naïve or *in vivo* poly(I:C) activated (250 µg I.P., 48 hours prior to isolation) NK cells were purified from WT, Ifnar1$^{-/-}$ or mice administered an Ifnar1 blocking antibody (MAR1-5A3, 200 µg I.P., 72, 48 and 24 hours prior to isolation) and co-cultured with calcein-AM labeled 4T1, 66cl4 or Yac-1 cells. After 4 hours the percentage of target cell lysis was quantified by detecting calcein released into the cell-free supernatants. (pooled NK cells from 3 mice were used in experiments with 3 technical replicates, repeated twice). Error bars represent SEM of all replicates. **(D - F)** Ifnar1$^{-/-}$ hosts bearing orthotopic 4T1 tumours were I.V. infused with 300,000 *in vivo* activated (250 µg poly(I:C) I.P., 48 hours prior to isolation) NK cells from WT or Ifnar1$^{-/-}$ donors on days 2, 7, 17 and 25 post tumour cell inoculation with primary tumours resected and weighed 15 days post tumour cell inoculation **(D)**. Metastatic burden in the lung **(E)** and spine **(F)** were quantified (black points) and overlayed on corresponding 4T1 metastasis data (from Figures 2B and 3A respectively, grey points, indicated in the key as 'whole animals') to give reference to the data distribution. Error bars represent SEM and *p*-value calculated using an unpaired t-test.

Figure 6.

NK cells initiate 66cl4 tumor cell apoptosis through agonism of the death-receptor pathway.

(A) 66cl4 and 4T1 tumor cells were analysed for the expression of Balb/c MHC class-I molecules (H2D(d), H2K(d)) as well as ligands for activating NK cell receptors (CD155, MULT1, Rae-1 and H60) and the type-1 IFN receptor (Ifnar1) by flow cytometry. Histograms are representative of two independent experiments. **(B)** *In vivo* stimulated NK cells (250 µg

I.P., 48 hours prior to NK isolation) from WT and Ifnar1$^{-/-}$ mice were purified and co-cultured with calcein-AM labeled 66cl4, 4T1 or Yac-1 cells for 18 hours. Target cell lysis was quantified by detecting calcein release into the supernantant (pooled NK cells from 2 mice were used in experiments with 3 technical replicates, repeated twice). Error bars represent SEM of all replicates. **(C)** Unlabelled 66cl4 cells were co-cultured with *in vivo* stimulated WT or Ifnar1$^{-/-}$ NK cells as described in (B). After 18 hours the remaining cells were stained with TO-PRO-3 and annexin-V-FITC to reveal the apoptotic population (TO-PRO-3^{+}/annexin-V^{+} cells) by flow-cytometery. Data are representative of two independent experiments.

Author Manuscript Published OnlineFirst on July 21, 2015; DOI: 10.1158/2326-6066.CIR-15-0065
Author manuscripts have been peer reviewed and accepted for publication but have not yet been edited.

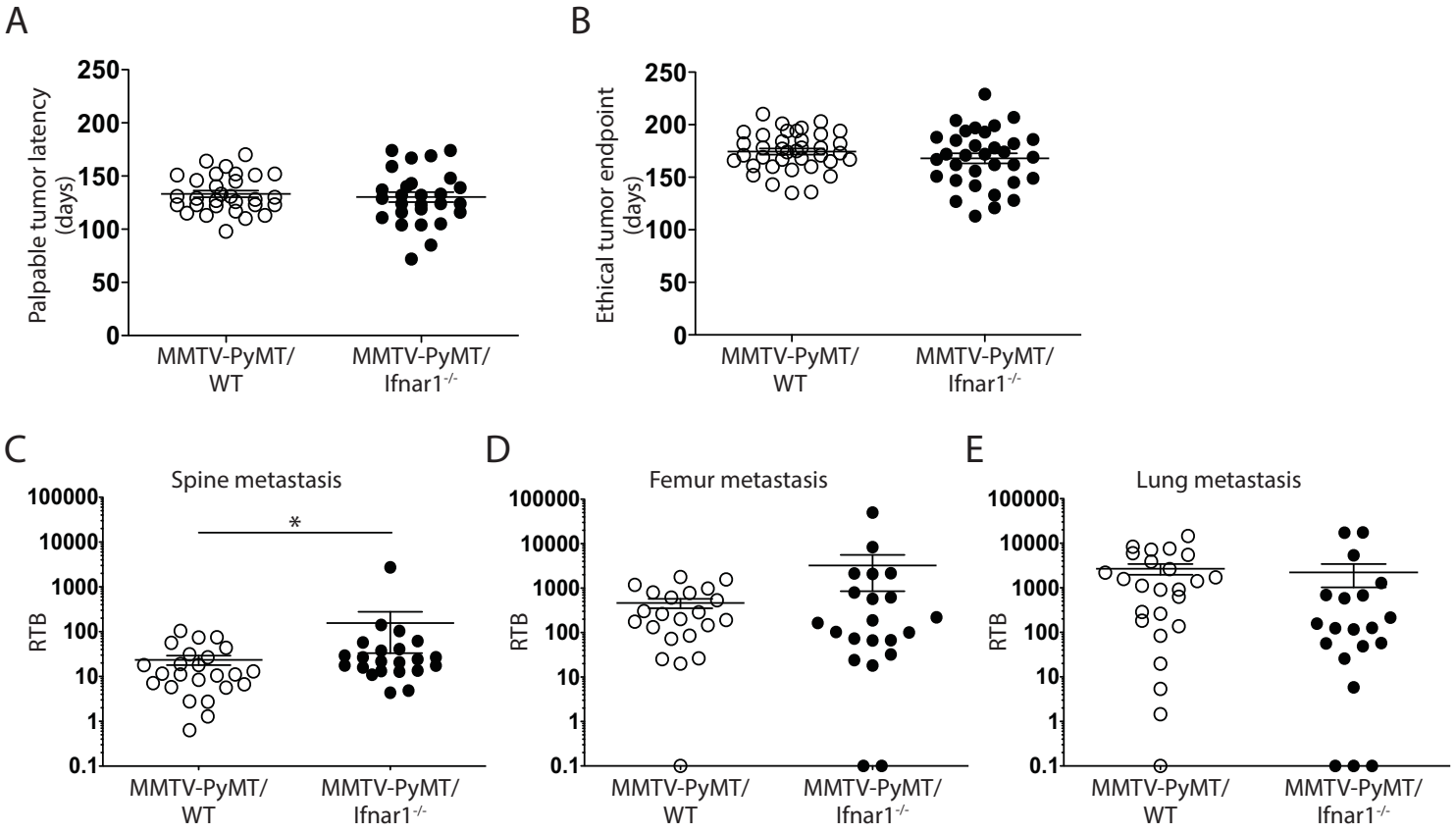

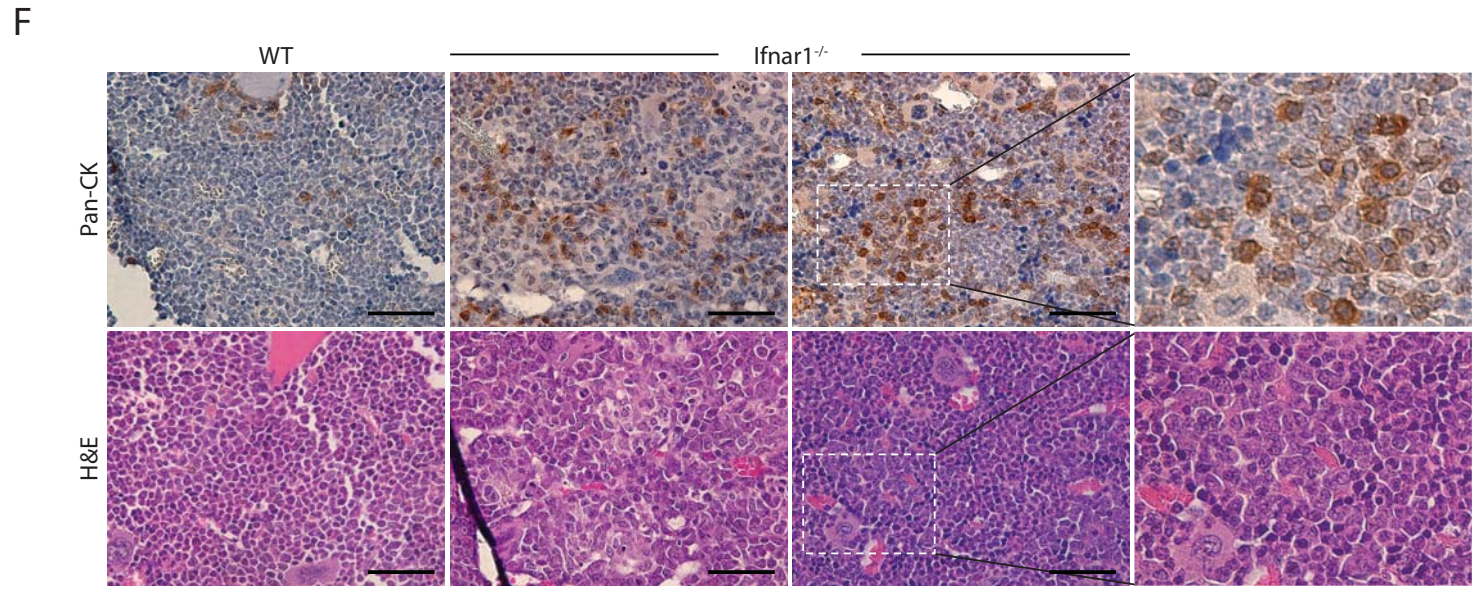

Figure 1

Author Manuscript Published OnlineFirst on July 21, 2015; DOI: 10.1158/2326-6066.CIR-15-0065
Author manuscripts have been peer reviewed and accepted for publication but have not yet been edited.

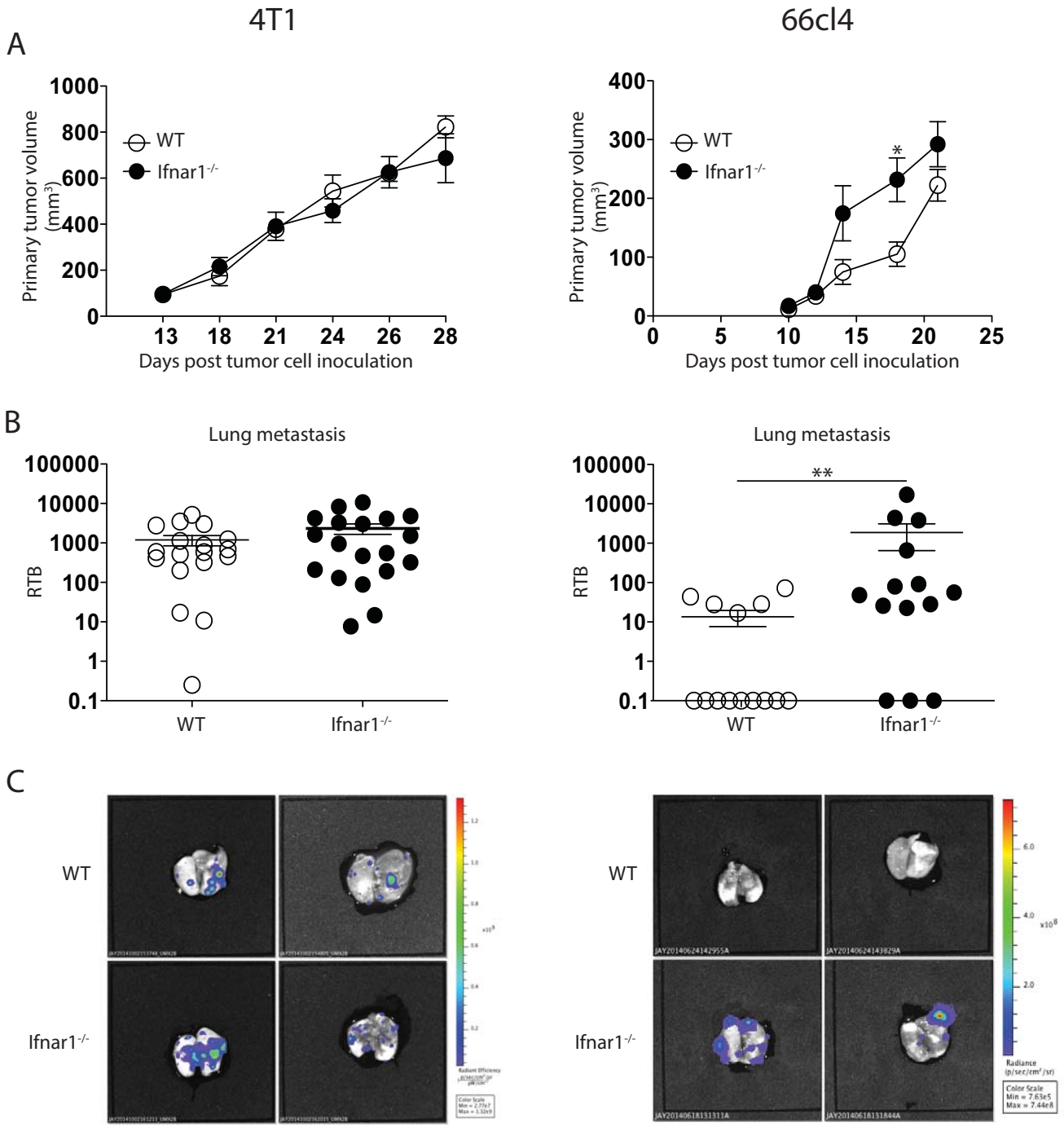

Figure 2

Author Manuscript Published OnlineFirst on July 21, 2015; DOI: 10.1158/2326-6066.CIR-15-0065
Author manuscripts have been peer reviewed and accepted for publication but have not yet been edited.

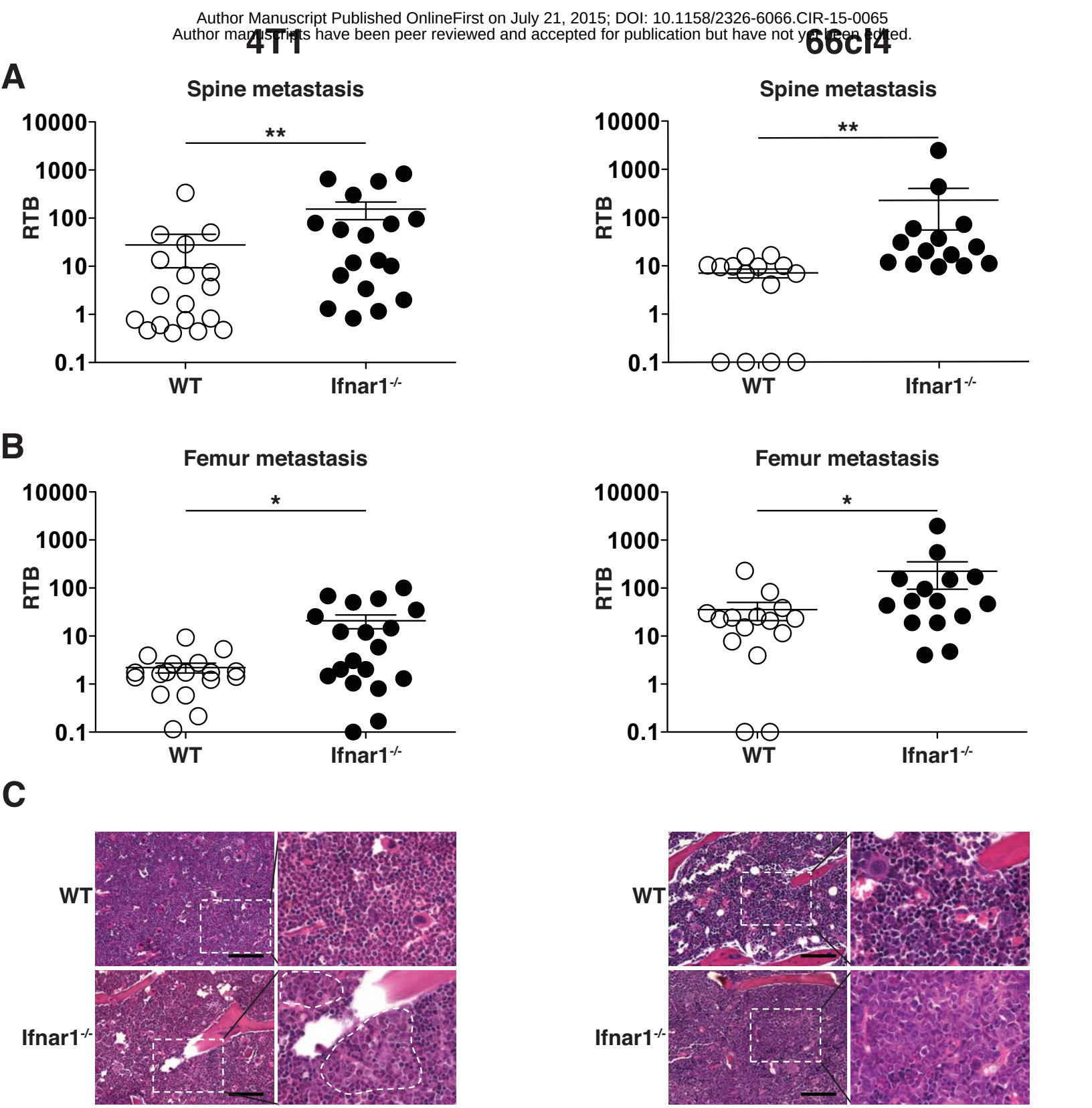

Figure 3

Author Manuscript Published OnlineFirst on July 21, 2015; DOI: 10.1158/2326-6066.CIR-15-0065
Author manuscripts have been peer reviewed and accepted for publication but have not yet been edited.

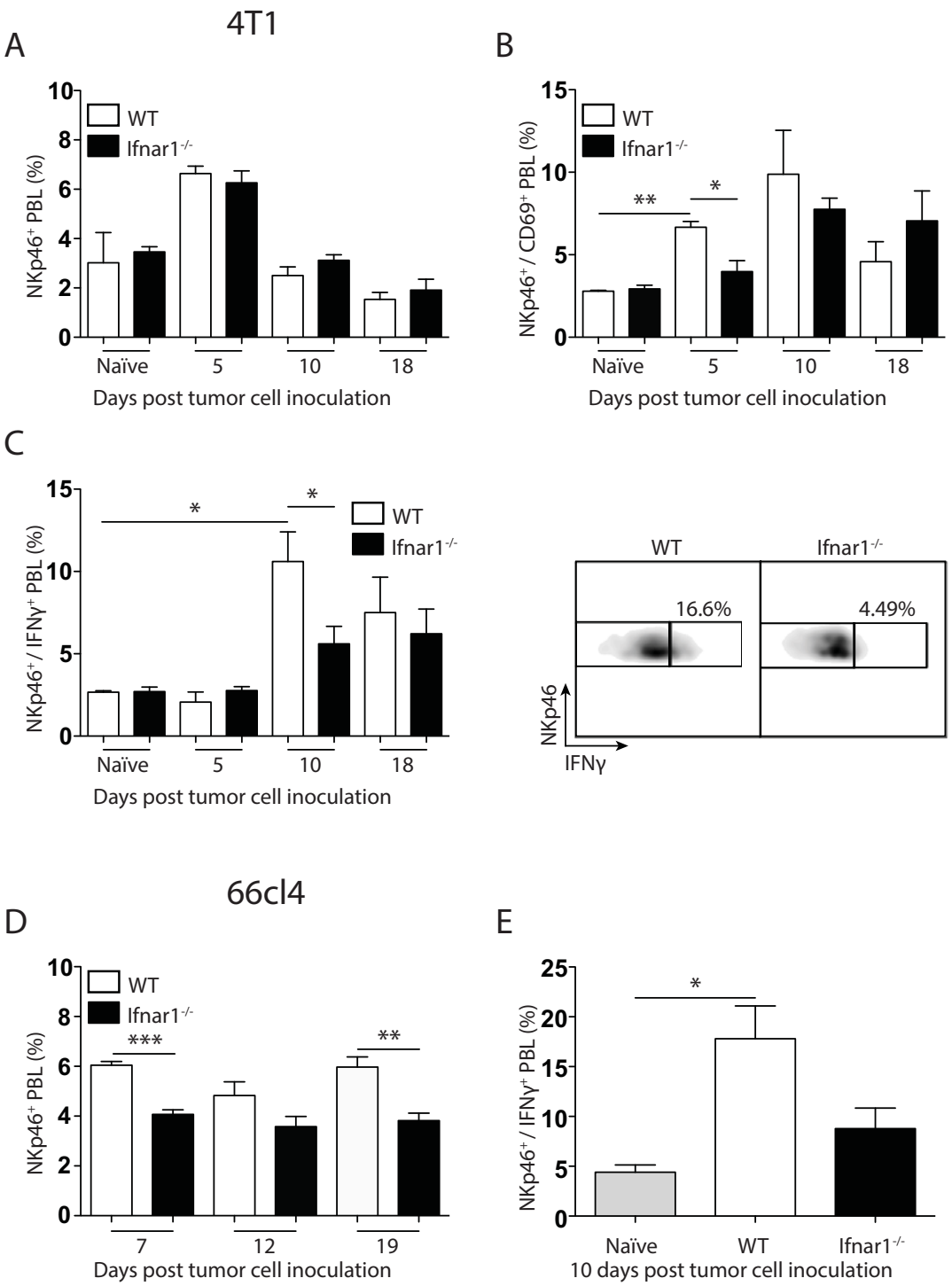

Figure 4

Author Manuscript Published OnlineFirst on July 21, 2015; DOI: 10.1158/2326-6066.CIR-15-0065
Author manuscripts have been peer reviewed and accepted for publication but have not yet been edited.

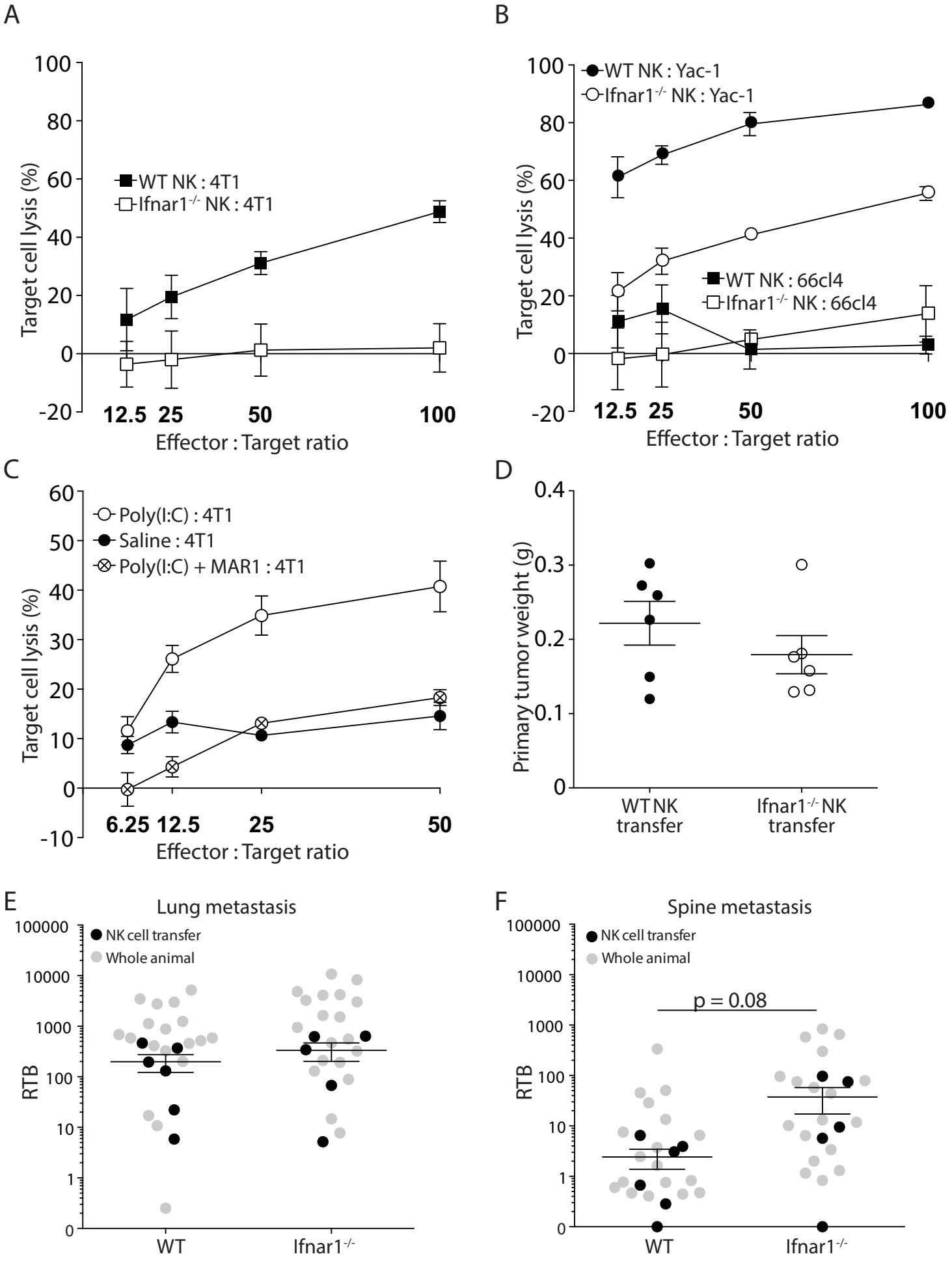

Figure 5

Author Manuscript Published OnlineFirst on July 21, 2015; DOI: 10.1158/2326-6066.CIR-15-0065
Author manuscripts have been peer reviewed and accepted for publication but have not yet been edited.

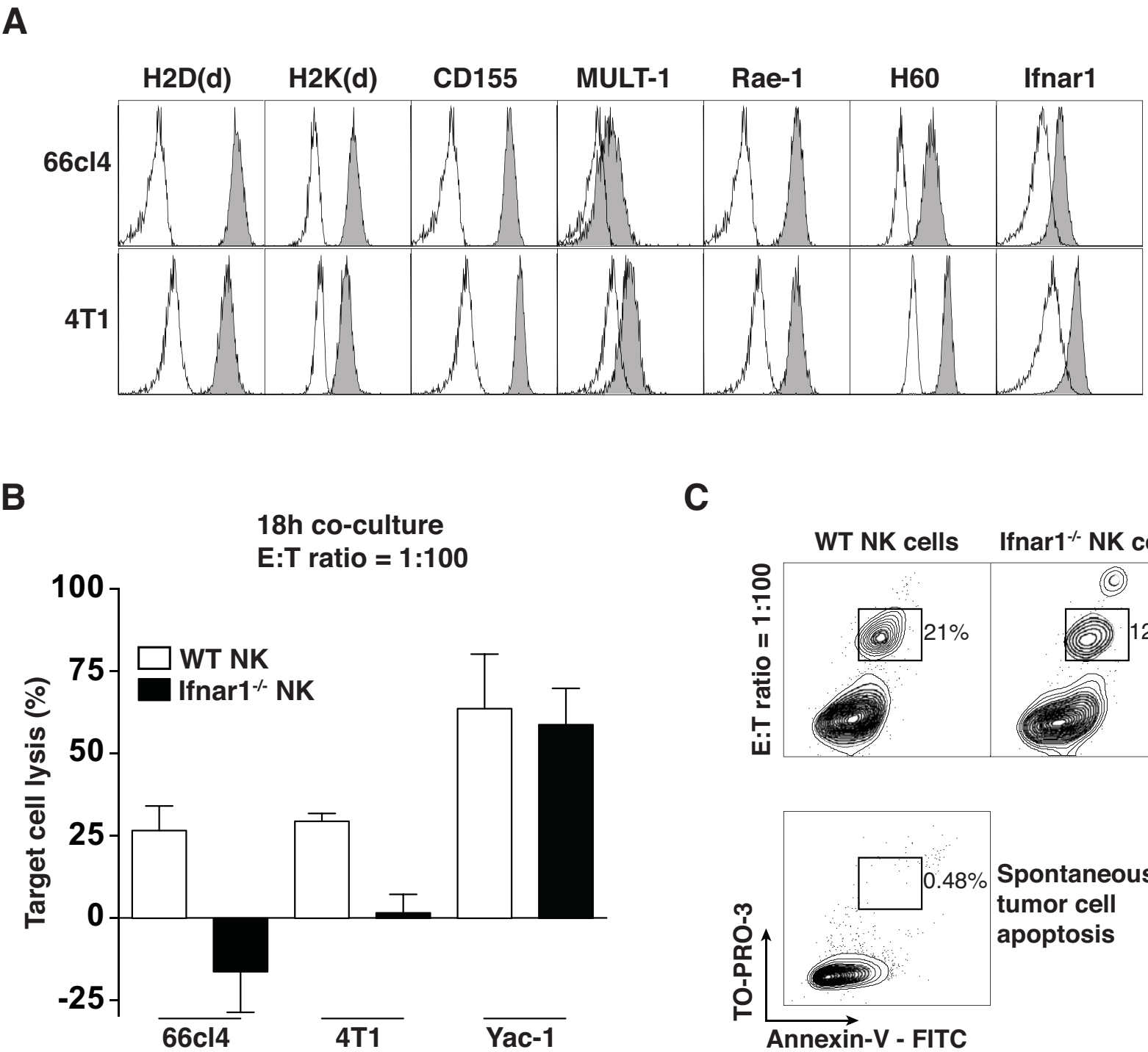

Figure 6

AACR American Association for Cancer Research

Cancer Immunology Research

Loss of host type-I IFN signaling accelerates metastasis and impairs NK cell anti-tumor function in multiple models of breast cancer

Jai Rautela, Nikola Baschuk, Clare Y Slaney, et al.

Cancer Immunol Res Published OnlineFirst July 21, 2015.